European Conference on Optical Communication (ECOC) 2022 © Optica Publishing Group 2022

InP/Si_3N_4 Hybrid External-Cavity Laser with sub-kHz Linewidth Acting as a Pump Source for Kerr Frequency Combs

Pascal Maier(1,2), Yung Chen(1), Yilin Xu(1,2), Matthias Blaicher(1,2), Dimitri Geskus(3), Ronald Dekker(3), Junqiu Liu(4), Philipp-Immanuel Dietrich(1,2,5), Huanfa Peng(1), Sebastian Randel(1), Wolfgang Freude(1), Tobias J. Kippenberg(4,6), Christian Koos(1,2,5,6)

(1) Institute of Photonics and Quantum Electronics (IPQ), Karlsruhe Institute of Technology (KIT), Germany
(2) Institute of Microstructure Technology (IMT), Karlsruhe Institute of Technology (KIT), Germany
(3) LioniX International B.V., Enschede, The Netherlands
(4) École Polytechnique Fédérale de Lausanne (EPFL), Lausanne, Switzerland
(5) Vanguard Automation GmbH, Karlsruhe, Germany
(6) Deeplight S.A., Lausanne, Switzerland

Abstract *We report on an InP/Si_3N_4 hybrid integrated ECL that relies on 3D-printed coupling elements such as intra-cavity photonic wire bonds and facet-attached microlenses. We demonstrate 90 nm tuning range, SMSR above 60 dB, and intrinsic linewidths of 979 Hz. We use the ECL as tunable pump laser for Kerr-comb generation.* ©2022 The Author(s)

Introduction

Tunable lasers are key building blocks of integrated optics. In this context, external-cavity lasers (ECL) are particularly interesting, opening the possibility to combine optical gain in III-V materials with tunable optical feedback offered by advanced photonic integrated circuits. Such feedback circuits can be efficiently implemented on the silicon photonic (SiP) platform [1–3], thereby offering a straightforward path towards monolithic co-integration with passive and active devices [4]. Alternatively, silicon nitride (Si_3N_4) can be used as base material for the feedback circuits [5–7], thereby overcoming the problem that achievable linewidths and power levels of SiP-based ECL are fundamentally limited through linear and nonlinear losses [5,8,9]. However, in both cases, the co-integration of III-V gain materials and tunable external-cavity circuits in a chip-scale package still represents a challenge. While wafer-bonding of InP epitaxial layers onto pre-processed passive waveguides (WG) paves a path towards highly scalable monolithic integration, the underlying processes are still comparatively complex [10] and largely limited to the SiP platform. Alternatively, ECL can be built from separate dies, which are combined on a package level. This approach allows the components to be optimized and tested individually and facilitates thermal decoupling of the gain element from the temperature-sensitive feedback circuit. However, hybrid multi-chip assembly of discrete dies conventionally requires high-precision alignment, thereby limiting fabrication throughput and scalability to high volumes.

In this paper, we demonstrate Si_3N_4-based hybrid integrated ECL that exploit photonic wire bonds (PWB) [1,11] for connecting reflective semiconductor optical amplifier (RSOA) elements to external-cavity circuits. In this approach, the dies are connected by a 3D-printed freeform waveguide that can be adapted to the positions and the mode-field sizes of the chips at either end. The concept does not require high-precision alignment and thus paves a path towards fully automated mass production. In our proof-of-concept experiments, we built hybrid ECL that combine intra-cavity PWB with 3D-printed facet-attached microlenses (FaML) [12,13] for coupling to fiber arrays. Our device offers a tuning range of 90 nm, side-mode suppression ratios (SMSR) above 60 dB, and intrinsic linewidths of 979 Hz – among the lowest values reported for comparable feedback architectures [2–7]. The viability of the ECL is demonstrated by using the device as narrow-linewidth tunable pump laser for Kerr frequency comb generation in high-Q Si_3N_4 microresonators.

Device Concept

The concept of a hybrid integrated ECL with 3D-printed intra-cavity photonic wire bond (PWB) and facet-attached microlenses (FaML) is shown in Fig. 1(a). The device consists of two dies – an InP RSOA and a Si_3N_4 (TriPleX) external-cavity circuit, which are connected by a polymer PWB. The Si_3N_4 chip is similar to the one described in [6] and comprises a cavity phase tuner (CPT), a tunable output coupler based on a Mach-Zehnder interferometer (MZI), as well as a Sagnac loop mirror with a pair of Vernier-type tunable racetrack resonators R1 and R2. The RSOA is 700 µm long, has a small-signal gain of 22 dB at a bias of 100 mA, and its saturation output power at λ = 1550 nm is P_{sat} = 11.4 dBm. The back facet features a high-reflectivity (HR) coating with a 90% power reflection. The front facet is angled at 9.0° and has an anti-reflection (AR) coating with respect to polymer. A PWB is used to connect the front facet to an edge coupler (EC) on the Si_3N_4 chip. This EC consists of a tapered WG which is oriented at an angle of 19.9° with respect to the facet normal. Note that the PWB allows to efficiently connect chips for which the emission angles are not matched, emphasizing the flexibility of the approach. The Si_3N_4 chip further comprises a 1 mm-long CPT and the Vernier pair of racetrack resonators with perimeters of 885.1 µm (R1) and 857.4 µm (R2). The CPT is used to adjust the cavity round-trip phase to an integer multiple of 2π at the wavelength corresponding to the maximum mirror reflectivity. The MZI-based tunable coupler is used to set the ratio between outcoupling from the laser cavity and feedback to the RSOA. Racetrack resonators, MZI, and CPT are tuned by thermal phase shifters. Four auxiliary WG (2-5) and the output WG (1) starting at the MZI, are routed to the Si_3N_4

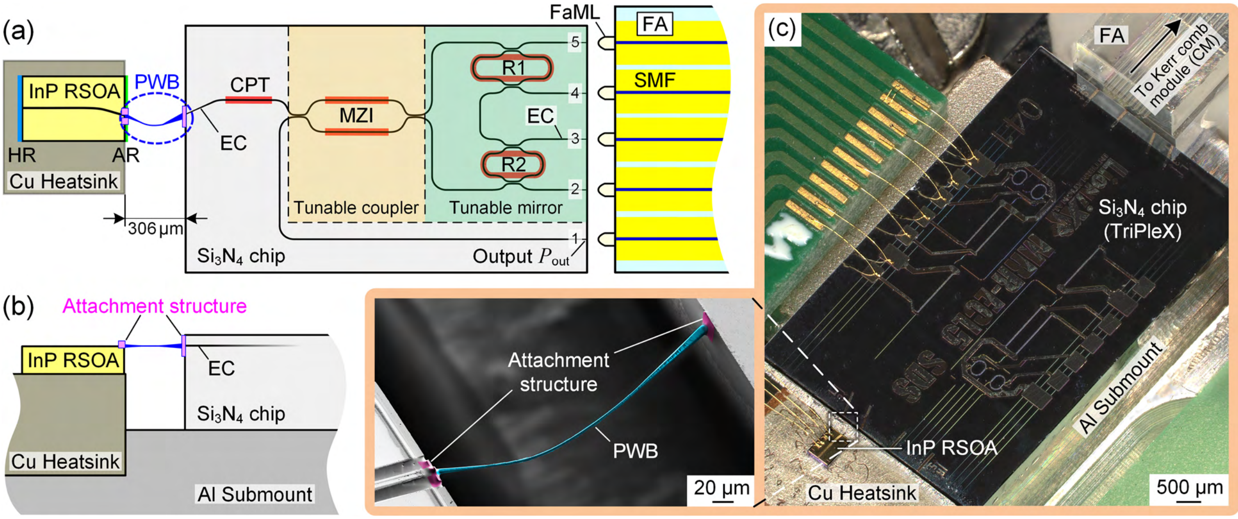

Fig. 1: Concept and implementation of a hybrid integrated ECL with 3D-printed intra-cavity photonic wire bond (PWB) and facet-attached microlenses (FaML). The device consists of two dies – an InP RSOA and a Si_3N_4 (TriPleX) external-cavity circuit, the latter comprising a cavity phase tuner (CPT), a tunable output coupler based on a Mach-Zehnder interferometer (MZI), and a Sagnac loop mirror with a Vernier pair of tunable racetrack resonators R1, R2. The RSOA back facet features a high-reflectivity (HR) coating with a 90% power reflection. The front facet is angled at 9.0° and has an anti-reflection (AR) coating with respect to polymer. A PWB connects the RSOA to an angled edge coupler (EC) on the Si_3N_4 chip. Attachment structures provide mechanical stability to the PWB. Four auxiliary WG (2-5) and the output WG (1) starting at the MZI, are routed to the Si_3N_4 chip edge opposite to the RSOA and connected to tapered EC with a pitch of 127 µm. A single-mode fiber (SMF) array (FA) with 3D-printed FaML is used to collect the light emitted from the waveguide facets (1-5). In a subsequent experiment, the emitted light is used to pump a Kerr-comb generator, see Fig. 3. **(a)** Schematic with building blocks. **(b)** Side-view of the coupling arrangement between RSOA and the Si_3N_4 chip. **(c)** Image of the assembled ECL along with a false-colored scanning electron microscope (SEM) image of the PWB (zoom-in).

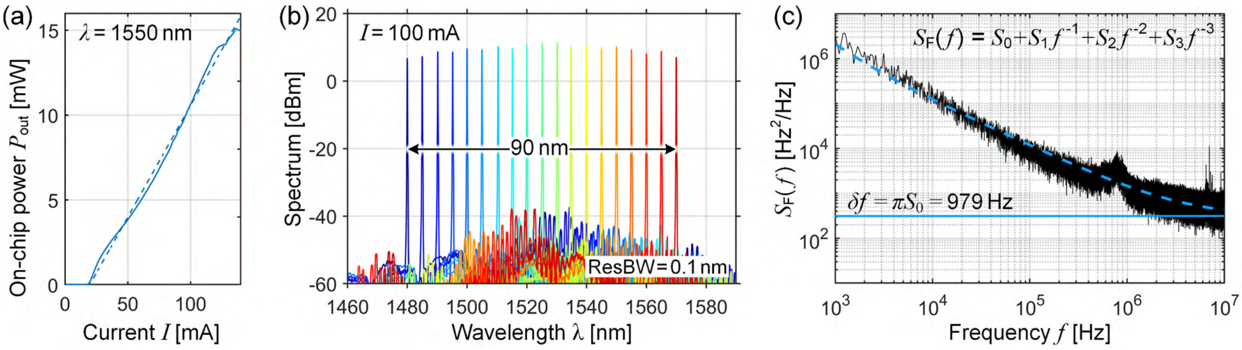

Fig. 2: ECL characterization. **(a)** Power P_{out} vs. injection current I for lasing at 1550 nm: threshold current 19 mA, slope efficiency 132 mW/A (fit by dashed straight line). **(b)** Superimposed ECL lasing spectra with tuning steps of 5 nm within the tuning range (1480…1570) nm for $I = 100$ mA. Maximum output power 12 dBm near 1530 nm. Side-mode suppression ratio SMSR > 50 dB, typically 60 dB. **(c)** FM noise spectrum with fit (blue dashed line). The intrinsic linewidth is $\delta f = 979$ Hz (solid blue line).

chip edge opposite to the RSOA and connected to tapered EC with a pitch of 127 µm. A single-mode fiber (SMF) array (FA) with 3D-printed FaML is used to collect the light emitted from the WG facets (1-5).

Module Assembly

In a first step, the RSOA is glued to a copper heatsink with an electrically conductive adhesive. The copper heatsink and the Si_3N_4 chip are then coarsely aligned to each other and glued to a common aluminium submount. Figure 1(b) provides a side-view of the module arrangement. The exact PWB trajectory depends on the chip positions and on the directions of the RSOA and the Si_3N_4 WG, see Fig. 1(a). The PWB comprises a taper with an initial widest cross-section of (4 × 4) µm, which is matched to the mode-field size at the RSOA facet. This cross-section is then reduced to the (2.4 × 2) µm cross-section of the curved PWB segment that is needed to adapt the non-matching emission angles of the two chips. A second PWB taper with a final cross-section of (8 × 5) µm is used to connect to the EC of the Si_3N_4 WG on the feed-back chip. Attachment structures on both chips provide mechanical stability to the PWB.

The PWB is made from a negative-tone resist (VanCoreA, Vanguard Automation GmbH, $n = 1.53$) by *in-situ* multi-photon lithography. The fabricated PWB is developed in propylene-glycol-methyl-etheracetate (PGMEA), flushed with isopropanol, and finally blow-dried. The five identical FaML on the FA are 3D-printed in a separate step for subsequent assembly with a custom pick-and-place machine. The lenses offer a working distance of 50 µm and are optimized for coupling to the mode-field diameter of the Si_3N_4 EC. Figure 1(c) shows a microscope image of the fully assembled ECL. A scanning electron microscope (SEM) image shows the false-colored PWB.

ECL Performance

The ECL wavelength is selected by aligning the two racetrack resonators to a common resonance, which may be detected through the two inner auxiliary WG (3, 4) in a loop-back configuration. Subsequently, the cavity phase and the tunable coupler are adjusted for maximum output power P_{out} emitted from the chip, see Fig. 1(a).

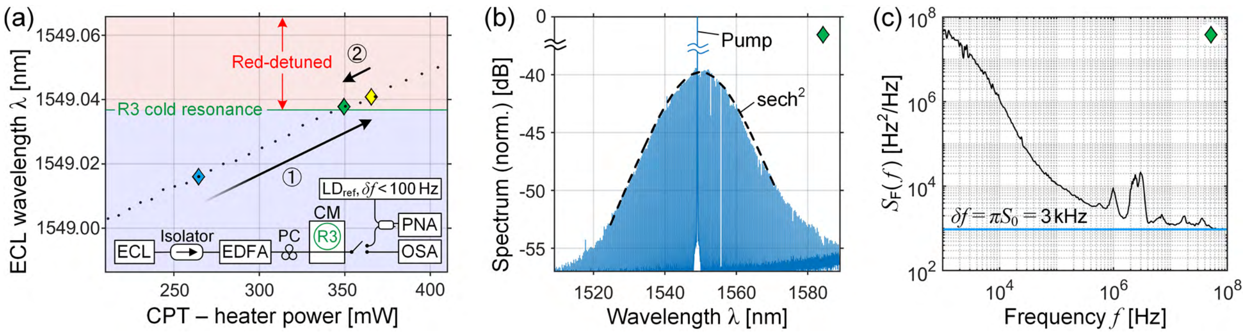

Fig. 3: Dissipative Kerr soliton (DKS) generation in a high-Q Si_3N_4 microresonator (R3) using the ECL as pump laser. **(a)** Setup and wavelength tuning of ECL by changing the heater power of the cavity phase tuner (CPT). The ECL wavelength is changed (arrow ①) from a blue-detuning (◆) with respect to the cold resonance wavelength of microresonator R3 (horizontal green line) to a red-detuned state (◆), where a multi-soliton state is observed. Then the ECL is tuned backwards (arrow ②), until a single-soliton state is reached at a pump wavelength slightly above the cold resonance of R3 (◆). Erbium-doped fiber amplifier (EDFA), polarization controller (PC), comb module (CM), phase noise analyzer (PNA) and reference laser (LD_{ref}, linewidth δf < 100 Hz), optical spectrum analyzer (OSA). **(b)** Spectrum of single-soliton DKS comb with a $sech^2$ envelope. The single-soliton state is indicated by a green diamond (◆) in (a). **(c)** FM noise spectrum of a typical single-soliton comb line, revealing an intrinsic linewidth of δf = 3kHz.

From the current-dependent emission power (PI curve) in Fig. 2(a) measured at a wavelength λ = 1550 nm, we extract a threshold current of 19 mA and a slope efficiency of 132 mW/A. We further estimate a PWB loss of 1.7 dB from measurements of the maximum emission power P_{out} = 9.6 dBm compared to the measured saturation output power P_{sat} = 11.4 dBm of the RSOA at the same wavelength and the same injection current. The mirror circuit contributes losses below 0.2 dB. Figure 2(b) depicts superimposed ECL lasing spectra with tuning steps of 5 nm within the tuning range (1480…1570) nm for I = 100 mA. A maximum output power of 12 dBm is measured at wavelengths near 1530 nm. SMSR are larger than 50 dB, typically 60 dB. We further measure the FM-noise spectrum of the ECL with a frequency discriminator (HighFinesse LWA-1k 1550). In this measurement, we adjust the tunable output coupler for minimum intrinsic linewidth. The associated FM-noise spectrum is shown in Fig. 2(c). From the fit of $S_F(f)$ (blue dashed line), an intrinsic linewidth of $\delta f = \pi S_0$ = 979 Hz is extracted.

Kerr Comb Generation

To demonstrate the viability of our integrated ultra-low linewidth ECL, we use the device as a tunable pump laser to generate a dissipative Kerr soliton (DKS) frequency comb. A schematic in the lower part of Fig. 3(a) depicts the setup: The ECL output is connected to an optical isolator and an erbium-doped fiber amplifier (EDFA). After a polarization controller (PC), the ECL pump is fed to a separately packaged comb module (CM). The CM comprises a Si_3N_4 ring resonator (R3, free spectral range 35.4 GHz), which is coupled to input and output fibers via PWB. The black dots in Fig. 3(a) illustrate how the ECL wavelength is tuned with the CPT heater power. The starting process of the DKS frequency comb is illustrated by three markers and two arrows: Starting with a blue-detuning (◆) of the ECL pump with respect to the cold resonance wavelength of R3 (horizontal green line), the ECL wavelength is increased (arrow ①) towards a red-detuning (◆), where a multi-soliton state is observed. Subsequently, the ECL pump is tuned backwards [14,15] (arrow ②), until at an ECL wavelength slightly above the cold resonance of R3 (◆) a single-soliton state is reached. For this state we record the spectrum with an optical spectrum analyzer (OSA), Fig. 3(b). The spectral envelope can be well approximated by a $sech^2$-characteristic. We also measure the FM-noise spectrum of a typical single-soliton comb line, Fig. 3(c), by superimposing it with a highly stable reference laser tone (LD_{ref}, δf < 100 Hz, NKT Photonics Koheras X15) on a photodetector, and by observing the photocurrent on a phase noise analyzer (PNA, R&S FSWP50). From this FM-noise spectrum, an intrinsic linewidth of δf = 3 kHz is found. To the best of our knowledge, this is the first demonstration of a single-soliton Kerr comb generated with a hybrid ECL as a pump source. Note that the Kerr comb generator used here features a threshold pump power of the order of (10…15) mW [16], which may be reduced further to below 5 mW [17]. Leveraging the full 15 mW of on-chip output power of the ECL would therefore allow to omit the EDFA and to integrate the pump ECL into the Kerr comb module similar to the demonstration in [17].

Summary

We demonstrate Si_3N_4-based hybrid integrated ECL that exploit PWB for connecting RSOA gain elements to external-cavity circuits. Without the need for high-precision alignment during assembly, a coupling loss of only 1.7 dB is achieved. Our approach combines the scalability advantages of monolithic integration with the performance and flexibility of hybrid multi-chip assemblies. The ECL features a tuning range of 90 nm between 1480 nm and 1570 nm, a maximum output power of 12 dBm, and typical side-mode suppression ratios above 60 dB. We measure an intrinsic linewidth of 979 Hz – among the lowest values reported for comparable feedback architectures. The viability of the ECL is demonstrated by using the device as narrow-linewidth tunable pump laser for Kerr frequency comb generation in high-Q Si_3N_4 microresonators.

Acknowledgements: DFG via the Excellence Cluster 3D Matter Made to Order (3DMM2O, EXC-2082/1 – 390761711) and in part by the DFG Collaborative Research Center WavePhenomena (SFB 1173, Project-ID 258734477); H2020 Marie Skłodowska-Curie Innovative Training Network MICROCOMB (#812818); BMBF projects Open6GHub (#16KISK010), DiFeMiS (#16ES0948), OPALID (#13N14589) and STARFALL (#16KIS1420); EU's Horizon 2020 research and innovation programme TeraSlice (#863322); ERC Consolidator Grant TeraSHAPE (#773248); Alfried Krupp von Bohlen und Halbach Foundation; Karlsruhe School of Optics & Photonics (KSOP).

References

1. Y. Xu, P. Maier, M. Blaicher, P.-I. Dietrich, P. Marin-Palomo, W. Hartmann, Y. Bao, H. Peng, M. R. Billah, S. Singer, U. Troppenz, M. Moehrle, S. Randel, W. Freude, and C. Koos, "Hybrid external-cavity lasers (ECL) using photonic wire bonds as coupling elements," Scientific Reports **11**(1), 16426 (2021), DOI: 10.1038/s41598-021-95981-w.

2. Y. Gao, J. Lo, S. Lee, R. Patel, L. Zhu, J. Nee, D. Tsou, R. Carney, and J. Sun, "High-power, narrow-linewidth, miniaturized silicon photonic tunable laser with accurate frequency control," Journal of Lightwave Technology **38**(2), 265–271 (2020), DOI: 10.1109/JLT.2019.2940589.

3. H. Guan, A. Novack, T. Galfsky, Y. Ma, S. Fathololoumi, A. Horth, T. N. Huynh, J. Roman, R. Shi, M. Caverley, Y. Liu, T. Baehr-Jones, K. Bergman, and M. Hochberg, "Widely-tunable, narrow-linewidth III-V/silicon hybrid external-cavity laser for coherent communication," Optics Express **26**(7), 7920 (2018), DOI: 10.1364/OE.26.007920.

4. M. A. Tran, D. Huang, J. Guo, T. Komljenovic, P. A. Morton, and J. E. Bowers, "Ring-resonator based widely-tunable narrow-linewidth Si/InP integrated lasers," IEEE Journal of Selected Topics in Quantum Electronics **26**(2), 1–14 (2020), DOI: 10.1109/JSTQE.2019.2935274.

5. K.-J. Boller, A. van Rees, Y. Fan, J. Mak, R. E. M. Lammerink, C. A. A. Franken, P. J. M. van der Slot, D. Marpaung, C. Fallnich, J. P. Epping, R. M. Oldenbeuving, D. Geskus, R. Dekker, I. Visscher, R. Grootjans, C. G. H. Roeloffzen, M. Hoekman, E. J. Klein, A. Leinse, and R. G. Heideman, "Hybrid integrated semiconductor lasers with silicon nitride feedback circuits," Photonics **7**(1), (2019), DOI: 10.3390/photonics7010004.

6. A. van Rees, Y. Fan, D. Geskus, E. J. Klein, R. M. Oldenbeuving, P. J. M. van der Slot, and K.-J. Boller, "Ring resonator enhanced mode-hop-free wavelength tuning of an integrated extended-cavity laser," Optics Express **28**(4), 5669 (2020), DOI: 10.1364/oe.386356.

7. Y. Guo, R. Zhao, G. Zhou, L. Lu, A. Stroganov, M. Nisar, J. Chen, and L. Zhou, "Thermally tuned high-performance III-V/Si_3N_4 external cavity laser," IEEE Photonics Journal **13**(2), (2021), DOI: 10.1109/JPHOT.2021.3068529.

8. B. Kuyken, F. Leo, S. Clemmen, U. Dave, R. Van Laer, T. Ideguchi, H. Zhao, X. Liu, J. Safioui, S. Coen, S. P. Gorza, S. K. Selvaraja, S. Massar, R. M. Osgood, P. Verheyen, J. Van Campenhout, R. Baets, W. M. J. Green, and G. Roelkens, "Nonlinear optical interactions in silicon waveguides," Nanophotonics **6**(2), 377–392 (2017), DOI: 10.1515/nanoph-2016-0001.

9. Y. Vilenchik, C. T. Santis, S. T. Steger, N. Satyan, and A. Yariv, "Theory and observation on non-linear effects limiting the coherence properties of high-Q hybrid Si/III-V lasers," in *Novel In-Plane Semiconductor Lasers XIV* (2015), p. 9382N, DOI: 10.1117/12.2078067.

10. D. Liang, A. W. Fang, H. Park, T. E. Reynolds, K. Warner, D. C. Oakley, and J. E. Bowers, "Low-temperature, strong SiO_2-SiO_2 covalent wafer bonding for III–V compound semiconductors-to-silicon photonic integrated circuits," Journal of Electronic Materials **37**(10), 1552–1559 (2008), DOI: 10.1007/s11664-008-0489-1.

11. M. Blaicher, M. R. Billah, J. Kemal, T. Hoose, P. Marin-Palomo, A. Hofmann, Y. Kutuvantavida, C. Kieninger, P.-I. Dietrich, M. Lauermann, S. Wolf, U. Troppenz, M. Moehrle, F. Merget, S. Skacel, J. Witzens, S. Randel, W. Freude, and C. Koos, "Hybrid multi-chip assembly of optical communication engines by in situ 3D nano-lithography," Light: Science & Applications **9**(1), 71 (2020), DOI: 10.1038/s41377-020-0272-5.

12. P. Maier, Y. Xu, M. Lauermann, A. Henniger-Ludwig, H. Kapim, M. Trappen, T. Kind, A. Weber, M. Blaicher, P.-I. Dietrich, C. Wurster, S. Randel, W. Freude, and C. Koos, "3D-printed optical elements for coupling of VCSEL and photodiode arrays to multi-core fibers in an SFP transceiver assembly," in *Optical Fiber Communication Conference (OFC) 2022* (Optica Publishing Group, 2022), p. W2A.1. DOI: 10.1364/OFC.2022.W2A.1.

13. P.-I. Dietrich, M. Blaicher, I. Reuter, M. R. Billah, T. Hoose, A. Hofmann, C. Caer, R. Dangel, B. J. Offrein, U. Troppenz, M. Moehrle, W. Freude, and C. Koos, "In situ 3D nanoprinting of free-form coupling elements for hybrid photonic integration," Nature Photonics **12**(4), 241–247 (2018), DOI: 10.1038/s41566-018-0133-4.

14. H. Guo, M. Karpov, E. Lucas, A. Kordts, M. H. P. Pfeiffer, V. Brasch, G. Lihachev, V. E. Lobanov, M. L. Gorodetsky, and T. J. Kippenberg, "Universal dynamics and deterministic switching of dissipative Kerr solitons in optical microresonators," Nature Physics **13**(1), 94–102 (2017), DOI: 10.1038/nphys3893.

15. P. Trocha, M. Karpov, D. Ganin, M. H. P. Pfeiffer, A. Kordts, S. Wolf, J. Krockenberger, P. Marin-Palomo, C. Weimann, S. Randel, W. Freude, T. J. Kippenberg, and C. Koos, "Ultrafast optical ranging using microresonator soliton frequency combs," Science **359**(6378), 887–891 (2018), DOI: 10.1126/science.aao3924.

16. J. Liu, H. Tian, E. Lucas, A. S. Raja, G. Lihachev, R. N. Wang, J. He, T. Liu, M. H. Anderson, W. Weng, S. A. Bhave, and T. J. Kippenberg, "Monolithic piezoelectric control of soliton microcombs," Nature **583**(7816), 385–390 (2020), DOI: 10.1038/s41586-020-2465-8.

17. B. Stern, X. Ji, Y. Okawachi, A. L. Gaeta, and M. Lipson, "Battery-operated integrated frequency comb generator," Nature **562**(7727), 401–405 (2018), DOI: 10.1038/s41586-018-0598-9.